JOURNAL OF GEOPHYSICAL RESEARCH, VOL. 111, C08020, doi:10.1029/2006JC003540, 2006

Directional spectra of hurricane wind waves

I. R. Young[1]

Received 10 February 2006; revised 2 June 2006; accepted 9 June 2006; published 29 August 2006.

[1] A comprehensive directional wave buoy data set showing the directional wave spectrum during the passage of a number of hurricanes is presented. The data confirm remote sensing measurements, showing that waves in the forward quadrants of the storm are dominated by swell radiating out from the intense wind regions to the right of the storm centre. The data show that for almost all quadrants of the storm, the dominant waves are remotely generated swell. The directional spectra are composed of swell at low frequency (the dominant waves) and locally generated waves above approximately three times the spectral peak frequency. There is, however, no tendency for the spectrum to become bi-modal in either frequency or direction. Rather, the spectra are directionally skewed, with a smooth directional transition from low frequency to high frequency. As for uni-directional wind field cases, the spectra are narrowest at the spectral peak frequency and broaden at frequencies above and below the peak. Despite the fact that much of the wave field is dominated by swell, the spectral width, as a function of non-dimensional frequency is very similar to that reported for uni-directional wind fields. The one-dimensional spectrum can be approximated by the parametric form proposed by Donelan et al. (1985). The parameters defining the spectrum also follow the same functional dependence as that reported for uni-directional winds. The fact that both the one-dimensional and directional spectra are very similar to spectra reported under simple uni-directional winds is interpreted as being a result of the shape stabilization effects of non-linear interactions. The data exhibit these same functional forms at low frequencies where they can be receiving no significant local input from the wind. This result indicates that the spectral shape is being controlled almost completely by the non-linear interactions with input and dissipation terms of lesser importance. This result indicates that input and dissipation are important in determining the total quantity of energy in the wave field, but appear to play only a minor role in determining the spectral shape.

Citation: Young, I. R. (2006), Directional spectra of hurricane wind waves, *J. Geophys. Res.*, *111*, C08020, doi:10.1029/2006JC003540.

1. Introduction

[2] Tropical cyclones, typhoons or hurricanes, represent the most extreme meteorological systems in tropical regions. These intense, geographically small systems typically generate wind speeds in excess of 40 m/s and significant wave heights above 10 m. A relatively extensive data set now exists of observations of the one-dimensional spectrum, wave height and period within such systems [e.g., *Ochi*, 2003; *Young*, 1997, 2003]. These data have been obtained from both in situ buoy and gauge measurements, as well as remote sensing data from aircraft and satellites. The corresponding data set of the directional properties within hurricanes is much more limited. In situ measurements using directional wave buoys and wave gauge arrays for a small number of storms exists [e.g., *Cardone and Pierson*, 1975; *Forristall et al.*, 1978; *Black*, 1979; *Forristall and Ward*, 1980]. More extensive remote sensing information, providing spatial coverage of the mean wave direction has been obtained by *Elachi et al.* [1977], *King and Shemdin* [1978], *Holt and Gonzalez* [1986], *Wright et al.* [2001] and *Walsh et al.* [2002]. These measurements do not however provide a detailed description of the directional spectrum suitable for oceanographic and engineering applications.

[3] This paper examines data recorded by directional buoys during the passage of 9 tropical cyclones off Australia's North-West coast (see Figure 1). Analysis of this data set enables the full directional wave spectrum to be resolved to frequencies as high as $5f_p$, where f_p is the frequency of the spectral peak. This data enables both the one-dimensional spectrum, the mean spectral direction and the directional spreading to be represented in a parametric form.

[4] The arrangement of the paper is as follows. In section 2, an overview of previous measurements of the

[1]Swinburne University of Technology, Melbourne, Victoria, Australia.

0148-0227/06/2006JC003540$09.00

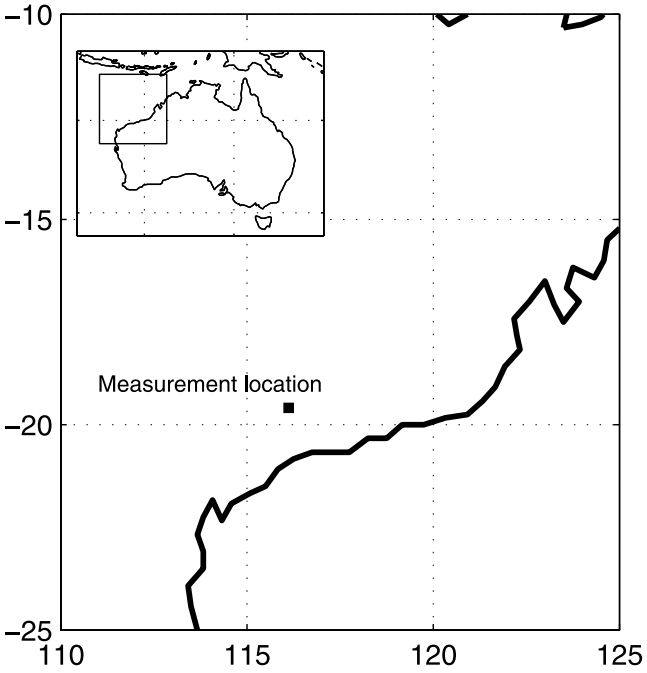

Figure 1. The measurement location at North Rankin platform on the North-West coast of Australia. The insert shows the map in relation to the continent of Australia.

directional wave field within hurricanes is presented. This is followed by a description of the present data set in section 3. Based on this data, an analysis of the directional wave field within typical hurricanes is presented in section 4. This analysis concentrates on the distribution of the dominant wave direction, relative to the central position of the hurricane. Section 5 presents an analysis of the directional spreading as a function of frequency and presents a parametric representation of this spreading. An analysis of the one-dimensional spectrum is presented in section 7 and a spectral form for hurricane waves proposed. Finally, conclusions and a discussion outlining the physical mechanisms which are believed responsible for the observed spectral forms, is presented in section 8.

2. Directional Wave Field in Hurricanes

[5] Intense tropical low pressure systems are typically termed, tropical cyclones, typhoons or hurricanes, depending on their geographical location. For simplicity, this paper will use the generic name hurricane to refer to such systems, irrespective of their physical location. In addition, unless the geographical location is important (e.g., Figure 2), all results are presented as though the storm is in the Northern Hemisphere (i.e. anti-clockwise circulation).

[6] Hurricane wind fields are characteristically intense, spatially inhomogeneous and directionally varying. The large gradients of wind speed and the rapid directional changes of the wind field lead to directionally complex wave fields within hurricanes. The well formed vortex of the hurricanes is, however, capable of being represented by relatively simple parametric models. A number of such models exist, a well known example being that of *Holland* [1980], who represented the gradient wind field as:

$$U_g = \left[\frac{AB(p_n - p_0)\exp(-A/r^B)}{\rho_a r^B} + \frac{r^2 f_c^2}{4}\right]^{0.5} - \frac{r f_c}{2} \qquad (1)$$

where U_g is the gradient wind (outside the atmospheric boundary layer) at radius r from the centre of the storm, f_c is the Coriolis parameter, ρ_a the air density, p_0 the central pressure, and p_n the ambient atmospheric pressure far from the storm. The parameters A and B can be expressed in terms of the radius to maximum winds, R, as

$$R = A^{1/B} \qquad (2)$$

The dimensionless parameter B defines the shape of the wind field with increasing distance from the centre of the hurricane. In the analysis that follows, it has been assumed that the winds spiral in towards the centre of the storm with a constant inflow angle of 25° [*Shea and Gray*, 1973]. Also, a first-order asymmetry has been applied by adding the hurricane velocity of forward movement to the symmetric flow [*Holland*, 1980]. Asymmetry of hurricanes is variable and some researchers have suggested adding only a fraction of the forward speed of the storm. An example of the wind field resulting from this relatively simple model can be seen in Figure 4b.

[7] A number of directional measurements of hurricane waves have been previously reported during the passage of individual storms, using a range of in situ instruments [e.g., *Cardone and Pierson*, 1975; *Forristall et al.*, 1978; *Black*, 1979; *Forristall and Ward*, 1980]. Although these measurements have provided valuable data, the spatial extent of the observations has been far too limited to provide a detailed understanding of the hurricane wave field. In contrast, measurements made using a variety of airborne or orbiting remote sensing instruments have provided a more comprehensive spatial understanding.

[8] The earliest such measurements were made for *Hurricanes Emmy*, *Francis* and *Gloria*, using an airborne Synthetic Aperture Radar (SAR) [*Elachi et al.*, 1977; *King and Shemdin*, 1978]. SAR measurements have also been made using orbiting satellites (e.g., Seasat and SIR-B), including measurements in *Hurricanes Iva* and *Josephine* and *Tropical Depression 12* [*Gonzalez et al.*, 1982; *Beal et al.*, 1986; *Holt and Gonzalez*, 1986]. More recently, *Wright et al.* [2001] and *Walsh et al.* [2002] have made comprehensive measurements for *Hurricane Bonnie* using a Scanning Radar Altimeter (SRA).

[9] From these studies, a consistent picture of the directional wave field can be developed. These observations show that ahead of the hurricane, the dominant waves radiate out from a region to the right (Northern Hemisphere) of the hurricane. Thus, at the measurement location, the local wind direction is often at angles up to 90° to the direction of propagation of the dominant waves. Therefore, it appears that these dominant waves have been generated in the intense wind regions to the right of the hurricane centre and have propagated ahead of the storm. In the rear quadrants, the situation is more confused, but again, the dominant waves are often at very large angles to the local

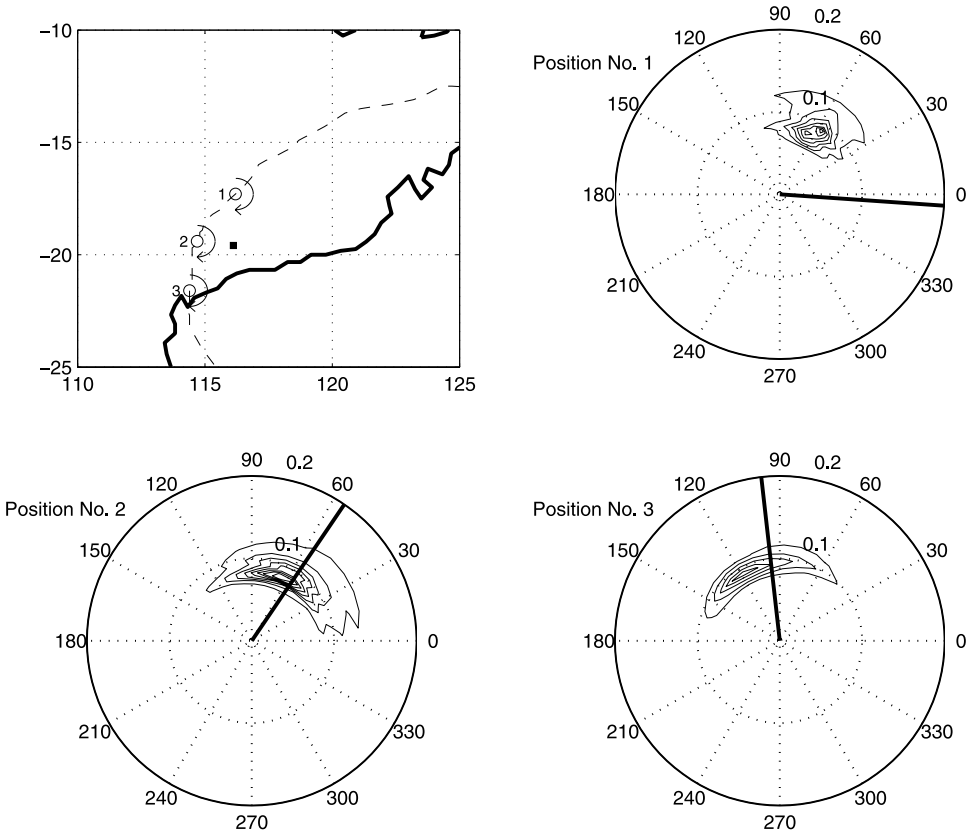

Figure 2. Recorded directional spectra measured during the passage of *T.C. Vance* past the measurement site at North Rankin platform in 1999. The upper left panel shows the measurement site (solid square), the coastline of Australia (thick line) and the track of *T.C. Vance* (dashed line). The position of the storm is marked at three points: Positions 1, 2 and 3 respectively. The remaining three panels show the directional spectra at each of these positions. Each directional spectrum has been normalized to have a maximum value of 1 and shown as polar contour plots. The radial axes of these plots are in units of [Hz]. The directional convention is that values are plotted as "coming from" the direction shown [i.e. 90° indicates coming from the top of the page]. The solid radial line shown on each panel represents the local wind direction at the time of the respective measurement. The spectra are shown for a Southern Hemisphere storm (i.e. clockwise circulation).

wind and appear to have propagated to the location of observation from near the centre of the translating hurricane. The SAR data is limited by the lack of a comprehensive SAR transfer function and the poor high frequency resolving power of the instrument. Hence, these measurements are limited to providing information on the mean direction of the dominant waves. The SRA data, however, provides a more comprehensive view of the directional spectrum, although the high frequency resolution is still limited. The data of *Wright et al.* [2001] indicate the dominant waves mentioned above have a narrow directional spread with observable energy within ±20° of the dominant direction. This observation is consistent with the conclusion that the dominant waves are remotely generated swell.

[10] Interestingly, these observations do not indicate that the directional spectra are bi-modal. There is no clear indication that, in addition to the remotely generated swell component, there is a significant locally generated sea, presumably intersecting with the swell at a significant angle. It should be noted, however, that this may simply be a result of the limitation of remote sensing instruments in imaging relatively short, high frequency waves.

[11] Based on this general concept of generation occurring in the intense wind regions of the translating hurricane, *King and Shemdin* [1978] proposed the concept of an "extended fetch" for hurricanes. This theory proposes that waves generated in the intense wind regions of the storm move forward with the storm, and hence experience an "extended fetch". In contrast, waves generated on the opposite side of the storm propagate in the opposite direction to the translation of the storm and the fetch is diminished. As a result, the intense wind region of the hurricane becomes the dominant area for wave generation, throughout the storm. *Young* [1988] and *Young and Burchell* [1996] confirmed this theory using numerical model simulations. They further extended the concept by demonstrating the "extended" (or equivalent) fetch is a function of both the maximum wind speed in the storm and the velocity of forward movement of the storm. For any given maximum wind speed, there will be a velocity of forward movement for which the waves generated will propagate with a group

velocity approximately equal to this velocity of forward movement. For this situation, the waves will remain in the intense wind region for the maximum period of time, and hence grow to a maximum magnitude. If the velocity of forward movement is reduced, the waves will propagate ahead of the storm, and if the velocity of forward movement is increased, the waves will be left behind the storm. In both cases, the equivalent fetch is reduced, as is the wave height. This concept has recently been termed ''the theory of trapped-fetch waves'' by *Bowyer and MacAfee* [2005].

[12] There have been numerous wave gauge/buoy measurements of one-dimensional spectra under hurricane forcing [e.g., *Whalen and Ochi*, 1978; *Ochi*, 1973, 1993; *Ross*, 1979; *Antani*, 1981; *Foster*, 1982; *Ochi and Chiu*, 1982; *Young*, 1997]. These spectra show two clear features. The spectral peak frequency tends to be relatively constant during the passage of a hurricane, even as the wind speed and wave height vary significantly. This is consistent with the previous observation that the wave field is dominated by swell radiating out from the centre of the storm. Within a distance of approximately $8R$ from the storm centre the spectra are uni-modal and visually similar to standard fetch-limited spectra. *Young* [1997] attributes this to the effects of nonlinear wave-wave interactions which transfer energy between the remotely generated swell and the local wind-sea in such a manner that the uni-modal form is preserved. This process has been termed the shape stabilization effect of nonlinear interactions [*Young and van Vledder*, 1993].

[13] A number of studies have attempted to fit standard parametric forms to these one-dimensional spectrum. These forms can be represented by the generalized JONSWAP form

$$F(f) = \beta g^2 (2\pi)^{-4} f_p^{-(5+n)} f^n \exp\left[\frac{n}{4}\left(\frac{f}{f_p}\right)^{-4}\right] \bullet \gamma^{\exp\left[\frac{-(f-f_p)^2}{2\sigma^2 f_p^2}\right]} \quad (3)$$

where $F(f)$ is the frequency spectrum (units m^2 s), β is a scale parameter, f_p is the spectral peak frequency, γ is a spectral peak enhancement factor and σ is a spectral width parameter. The parameter n represents the slope of the high-frequency face of the spectrum. For a value of $n = -5$, (3) reverts to the standard JONSWAP form of *Hasselmann et al.* [1973] and for $n = -4$ to the form proposed by *Toba* [1973] and *Donelan et al.* [1985].

[14] *Young* [1997] considered an extensive database from tropical cyclones on the North-West coast of Australia and found that within the data scatter, either of the forms mentioned above could equally well represent the data. Further, it was found that the spectral parameters could be represented as functions of the inverse wave age, U_{10}/C_p, where U_{10} is the wind speed measured at a height of 10 m and C_p is the phase speed of waves at the spectral peak frequency. Surprisingly, these relationships were consistent with forms developed for fetch limited spectra. Again, they attributed this to the shape stabilization effect of non-linear wave-wave interactions. *Ochi* [1993] fitted the JONSWAP form to North American hurricane data and represented the parameters by relationships in terms of H_s and f_p, where H_s is the significant wave height. *Young* [2003] reformulated these relationships, showing that they were consistent with the formulations of *Young* [1997], expressed in terms of U_{10}/C_p. Hence, the data sets of *Ochi* [1993] and *Young* [1997] were consistent, despite the fact that they were from different geographical regions.

[15] The relationships of *Young* [1997] show that typical hurricane spectra have inverse wave ages near 1 and values of peak enhancement factor, γ between 1 and 2. These values are typical of relatively mature wind-wave spectra. This is not surprising when it is remembered that the wave field is dominated by swell generated remotely, in regions of high winds. Once this energy has propagated into regions where the local wind is lower than the generation region, the resulting values of U_{10}/C_p will be low and hence the waves in such cases can be described as ''mature'' (i.e. low U_{10}/C_p and low γ).

3. Hurricane Database

[16] The database considered in this paper consists of measurements made by Datawell directional wave buoys on Australia's North-West shelf. Data from a total of 9 hurricanes over the period 1995–2000 was considered. The data was recorded at Woodside Petroleum's North Rankin platform in approximately 130 m water depth (see Figure 1). The parameters representing the hurricane wind fields for these storms, (1) have been carefully evaluated in separate studies by Woodside and validated against Australian Bureau of Meteorology wind and surface pressure observations. As such, the tracks and wind fields associated with these hurricanes are of good quality. Further tests of the model represented by (1) where made against anemometer data at North Rankin and found to be reliable [wind speed typically ±15% and direction ±15°]. As anemometer data was not available for all the storms, model predictions from (1) for U_{10}, have been adopted for the remainder of this study. This is the same approach adopted by *Young* [1997].

[17] The Datawell directional buoy measures three orthogonal components of acceleration, from which co- and quad-spectra of the displacements can be formed: C_{hh} the co-spectrum of the vertical displacement, C_{xx} the co-spectrum in the horizontal x direction, C_{yy} the co-spectrum in the horizontal y direction and the respective quad-spectra Q_{hx}, Q_{hy} and Q_{xy}. Hence, the buoy provides 6 quantities, related to the two-dimensional wave field. The full two-dimensional (frequency-direction) spectrum requires the spectrum to be defined throughout this two-dimensional domain (perhaps hundreds of points). Therefore, the spectrum typically has many more degrees of freedom than there are independent measured quantities. In order to make the problem tractable, simplifying assumptions are required.

[18] There are three common approaches to the analysis of such data. The Fourier Expansion Method (FEM) was proposed by *Longuet-Higgins et al.* [1963] and assumes that the directional spectrum conforms to a pre-determined form, typically $\cos^{2s}(\theta/2)$, where s is a parameter determining the spreading width. A number of other techniques which avoid the need to adopt a pre-determined spreading form have also been proposed, including the Maximum Likelihood Method (MLM) [*Capon*, 1969; *Isobe et al.*, 1984] and the Maximum Entropy Method (MEM) [*Lygre and Krogstad*, 1986]. A comparison of these various approaches has been presented by *Young* [1994], who conclude that the MLM provides a good compromise between relatively high directional re-

solving power and the ability to resolve multiple directional wave trains, whilst avoiding the generation of spurious peaks. The ability to resolve bi-modal directional distributions at a particular frequency is particularly relevant to hurricane spectra, where multiple wave components might be expected to occur. For this reason, the MLM was adopted for this study.

[19] The directional wave spectrum, $E(f, \theta)$ can be defined as [*Longuet-Higgins et al.*, 1963]:

$$E(f,\theta) = F(f)D(f,\theta) \tag{4}$$

where $D(f, \theta)$ is a directional spreading function, constrained such that $\int D(f, \theta)d\theta = 1$. Following *Isobe et al.* [1984] the spreading function can be determined using MLM as:

$$D(f,\theta) \approx [M_0 M_2\left(\xi^2 \cos^2\hat{\theta} + \sin^2\hat{\theta}\right) - M_1^2 \sin^2\left(\hat{\theta} - \hat{\theta}_m\right) - 2M_1 M_2\left(\xi^2 \cos\hat{\theta}\cos\hat{\theta}_m + \sin\hat{\theta}\sin\hat{\theta}_m\right) + M_2^2\xi^2]^{-1} \tag{5}$$

where

$$M_0 = C_{hh} \tag{6}$$

$$M_1 = \sqrt{Q_{hx}^2 + Q_{hy}^2} \tag{7}$$

$$M_2 = \frac{C_{xx} + C_{yy}}{2} + \sqrt{\left(\frac{C_{xx} - C_{yy}}{2}\right)^2 + Q_{xy}^2} \tag{8}$$

$$\hat{\theta} = \theta - \theta_p \tag{9}$$

$$\hat{\theta}_m = \theta_m - \theta_p \tag{10}$$

$$\theta_m = \tan^{-1}\left(\frac{Q_{hy}}{Q_{hx}}\right) \tag{11}$$

$$\theta_p = \frac{1}{2}\tan^{-1}\left(\frac{2Q_{xy}}{C_{xx} - C_{yy}}\right) \tag{12}$$

$$\xi^2 = \frac{\left(C_{xx} + C_{yy}\right) - \sqrt{\left(C_{xx} - C_{yy}\right)^2 + 4Q_{xy}^2}}{\left(C_{xx} + C_{yy}\right) + \sqrt{\left(C_{xx} - C_{yy}\right)^2 + 4Q_{xy}^2}} \tag{13}$$

and θ_m is the mean wave direction, θ_p is the principle wave direction and ξ is a long-crestedness parameter. Note that in (6) to (13), each of the quantities is also a function of frequency, f.

[20] Spectra were also analysed using the simpler FEM and compared with the results of (5). In almost all cases, the results were similar, with the MLM giving slightly narrower directional spreading. This is consistent with the results of *Young* [1994], who showed that directional spectra obtained using the FEM are artificially broad.

[21] Figure 2 shows contour plots of the directional spectrum, analysed using MLM during the passage of *T.C. Vance* past the North Rankin measurement site. The storm track, together with the spectra for three positions during the passage of the tropical cyclone past the measurement site are shown. Also shown is the direction of the local wind, at the measurement site at the time of each of the measured spectra. Note that this is a Southern Hemisphere storm and is shown as such, as the geography is important in this figure. Therefore the wind circulation is clockwise around the storm centre.

[22] A number of features of the directional spectra are clear in this figure. As the storm approaches the measurement site (Position No. 1), waves appear to radiate out from the centre of the storm. The angle between the local wind and the direction of propagation of the dominant waves is approximately 60°. As the storm passes to the west of the measurement location (Position No. 2), the local wind and dominant wave directions align (close to the most intense wind region of the storm). As the storm passes the measurement site (Position No. 3), the local wind rotates anti-clockwise and the dominant wave direction also rotates in this same direction. There is a suggestion that the directional width of the spectrum is narrower as the storm approaches the site (e.g., Compare Position No. 1 with both other cases). Such a result would be consistent with the spectrum being composed largely of swell at Position No. 1 and more locally generated wind-sea at the other positions.

[23] In this region of the Indian Ocean there is a persistent swell from the south-west (Southern Ocean). In the summer months, when these data sets were recorded, this swell energy is relatively small. The swell is detected by the MLM analysis, however, provided the hurricane is within $10R$, the hurricane generated wave field dominates. As a result, this swell energy is not apparent in any of spectra shown in this paper.

4. Directional Properties of the Spectra

[24] The passage of each of the hurricanes past the measurement site effectively provides one transect through the spatial hurricane wave field. Therefore, by combining all hurricanes within the database, a relatively comprehensive understanding of the full directional wave field within a hurricane can be developed. For each of the hurricanes within the database, and at each time for which there is a recorded directional spectrum, the direction of forward propagation and velocity of forward movement were used to transform the data into a frame of reference moving with the hurricane. In this moving frame of reference, the location of the measurements moves relative to the centre of the storm and marks out a transect across the spatial wave field. As the spatial scale of each storm differs, all spatial dimensions were normalized in terms of the radius to maximum winds, R. In addition, the data was transformed, such that it is applicable to a Northern Hemisphere storm (i.e. anti-clockwise circulation). That is, all directions were "mirror imaged" about the direction of forward movement of the storm.

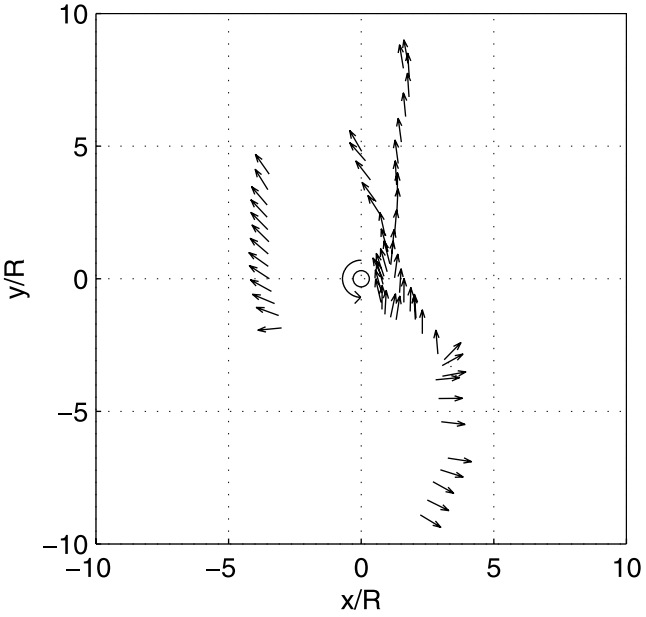

Figure 3. Vectors showing the dominant wave direction for three of the hurricanes. The data are shown in a transformed co-ordinate system moving with the hurricane, with the direction of propagation towards the top of the page. The storm centre is shown by the open circle at co-ordinates 0,0. The spatial co-ordinates are shown scaled by the radius to maximum winds, R. The system is shown for the Northern Hemisphere (i.e. anti-clockwise circulation).

[25] As will be shown later, the spectra are typically not bi-modal, and hence a dominant direction of propagation can be clearly assigned to each spectrum. This was achieved by defining the dominant wave direction, $\bar{\theta}$, by the weighted integral

$$\bar{\theta} = \tan^{-1}\left[\frac{\int\int E(f,\theta)^4 \sin(\theta) df\ d\theta}{\int\int E(f,\theta)^4 \cos(\theta) df\ d\theta}\right] \quad (14)$$

The exponent "4" in (14) is arbitrary and weights the result to the most energetic region of the spectrum. Experimentation with a range of values showed that the outcome was largely insensitive to the choice of the value.

[26] Figure 3 shows values of $\bar{\theta}$ in the rotated and normalized frame of reference for three of the hurricanes. In this frame of reference, the hurricane is propagating towards the North (top of page). The hurricane track was smoothed using a running 3-point filter, so as to avoid unrealistic rotations of the storm, brought about by short-scale variations in the track position. The passes shown in Figure 3 clearly show the dominant waves radiating out from near the centre of the hurricane.

[27] The values of $\bar{\theta}$ for each of the storms were combined by "binning" each of the individual values into $1R \times 1R$ squares and averaging the values in each of the squares. The resulting distribution of dominant wave directions is shown in Figure 4a, with a typical wind field shown in Figure 4b, for comparison. As pointed out by *Young* [1988], the detailed directional distribution of waves within a hurricane depends, to some extent, on parameters such as the velocity of forward movement, V_{fm} and the maximum wind speed in the storm, $V_{\max}$. Figure 4a ignores such influences, as it averages all the storms in the database, irrespective of these factors. In addition, fluctuations in the magnitudes of V_{fm} and $V_{\max}$ will impact on the wave field, such variability being filtered out in the present analysis. As a result, some of the variability in the results may be due to these influences. Nevertheless, the figure provides a first-order estimate of the two-dimensional directional properties of waves in a hurricane. Many of the features previously inferred from remote sensing data and numerical models are clear from this composite of in situ measurements.

[28] Waves in both the left and right forward quadrants and the left rear quadrant radiate out from a region to the right of the storm centre. In the right rear quadrant, the waves more closely align with the local wind direction. This pattern is consistent with previous suggestions that dominant waves radiated out from an area near the intense wind "crescent" of the hurricane, as shown in Figure 4b. Comparison of Figures 4a and 4b shows that throughout much of the hurricane, the difference between the wind direction and direction of propagation of the dominant waves is very large, approaching 90°.

[29] As can be seen in Figure 4a, data are confined to a region of approximately $\pm 10R$ ahead of and behind the centre of the hurricane and $\pm 5R$ either side of the storm. This is a significant area and covers the major area of

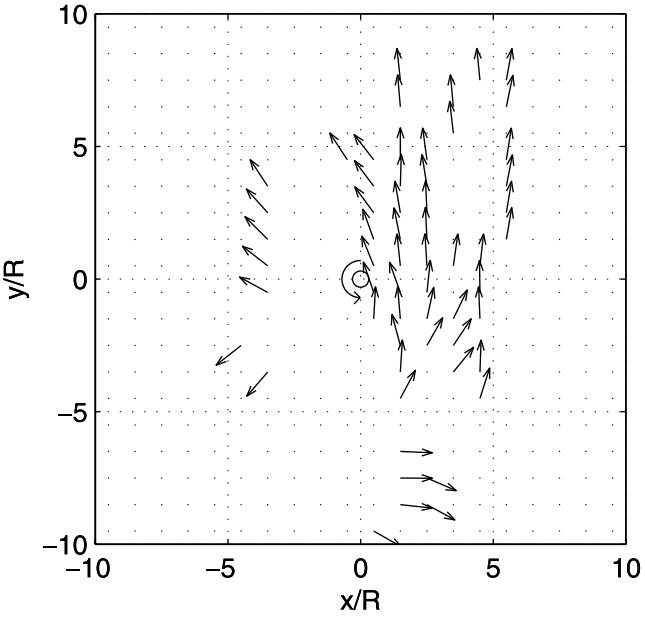

Figure 4a. A composite of all storms in the database showing the mean values of the dominant wave direction in squares of size $1R \times 1R$. Areas with no vectors shown correspond to squares where there were insufficient measurements to form a reliable estimate of dominant wave direction. The hurricane centre is shown by the open circle at co-ordinates 0,0. The system is shown for the Northern Hemisphere (i.e. anti-clockwise circulation).

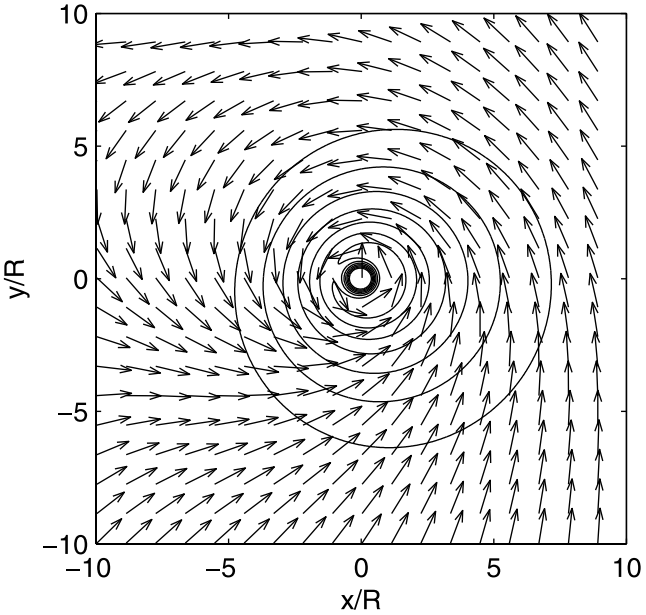

Figure 4b. A typical wind field for a Northern Hemisphere hurricane, as predicted by the model (1). The contours are of wind speed, U_{10}, with the vectors showing wind direction. The scale is identical to Figure 4a. The system is shown for the Northern Hemisphere (i.e. anticlockwise circulation).

significant winds in a hurricane. Nevertheless, the conclusions reached in this work are valid only in this domain.

5. Directional Spreading Functions

[30] A more detailed understanding of the directional properties of the hurricane spectra can be gained by examination of the directional spreading function, $D(f, \theta)$, as defined in (4). Figure 5 shows examples of $D(f, \theta)$, for each of the four quadrants of the hurricane. The spreading functions are shown as contour plots as functions of f/f_p and θ. At each frequency, D has been normalized to a maximum value of 1. These figures clearly show that the spectra are directionally skewed. At the spectral peak ($f/f_p = 1$), the spectrum is aligned with the dominant wave direction, as shown in Figure 4a. With increasing frequency, the spectrum gradually rotates towards the local wind direction. By $f/f_p \approx 3$, the spectrum is aligned with the local wind direction.

[31] As with directional spectra recorded under uni-directional wind fields [e.g., *Mitsuyasu et al.*, 1975; *Hasselmann et al.*, 1980; *Donelan et al.*, 1985; *Babanin and Soloviev*, 1998], the spectra are narrowest at $f/f_p \approx 1$ and broaden at frequencies both above and below the spectra peak frequency. Noting that it was hypothesised above, that the components at the spectral peak were remotely generated swell, it is clear from Figure 5 that this swell and the high frequency, locally generated wind-sea are coupled. There is a smooth transition between the two systems and no tendency to generate separate bi-modal peaks. There appears to be a continuous feed of energy from one system to the other. This is presumably due to non-linear wave-wave interactions, as discussed in section 8.

[32] The one-dimensional frequency spectrum is also shown for each case in Figure 5 (centre panels). In all cases, this spectrum is uni-modal. Coupled with the form of the directional spreading function, this confirms that there is no tendency for the directional spectrum to be bi-modal.

[33] In addition to the contour plots of the directional spreading function and the one-dimensional spectra, Figure 5 also shows the position of the measurement site, relative to the hurricane centre (expressed in terms of R), the dominant wave direction and the local wind direction are also shown. Based on the dominant wave direction, the figure also provides an estimate of the probable generation region for the waves at the peak of the spectrum (remote swell), and the position of the hurricane at the time of generation. This point of origin is only approximate and has been obtained by backward ray tracing.

5.1. Left-Forward Quadrant

[34] Figure 5a shows a case from the left-forward quadrant. The difference in direction between the local wind and dominant waves is approximately 130°, but the local wind-sea does not appear well aligned with the model estimate of the wind direction. The difference in direction between the local wind-sea and the dominant waves is approximately 90°. It is reasonable to conclude that the model prediction of local wind direction is not particularly accurate for this case. This is not surprising, as the model assumes a rather simplistic constant inflow angle for the wind direction. Therefore, it is likely that the wind direction is less accurate than the wind speed, for which the model has been much more extensively calibrated. Tracing back the dominant waves to their likely point of origin, it appears that they were generated in the right-forward quadrant of the storm, just ahead of the intense wind crescent. Such a generation region is logical, as waves generated in the intense wind crescent could not propagate into the left-forward quadrant. Therefore, the generation region just ahead of this crescent represents the area with the most intense winds, capable of producing waves which could propagate to the measurement site.

5.2. Right-Forward Quadrant

[35] Figure 5b shows a case from the right-forward quadrant. The difference in direction between the local wind and the dominant waves is approximately 60°, with the waves being largely aligned with the local wind above $2.5f_p$. The dominant waves appear to have been generated in the intense wind crescent to the right of the storm centre and have propagated more rapidly than the storm to arrive at the measurement location, significantly ahead of the storm.

5.3. Right-Rear Quadrant

[36] Figure 5c shows a case for the right-rear quadrant. In this region, the wind-sea and the dominant waves are more closely aligned, differing only by approximately 30°. It appears that the dominant waves in this region are largely generated locally, rather than being remotely generated swell. This is consistent with the wind pattern within the hurricane, with no obvious remote generation region existing for this quadrant. It also appears that the directional spreading is broader for this case. This would be consistent

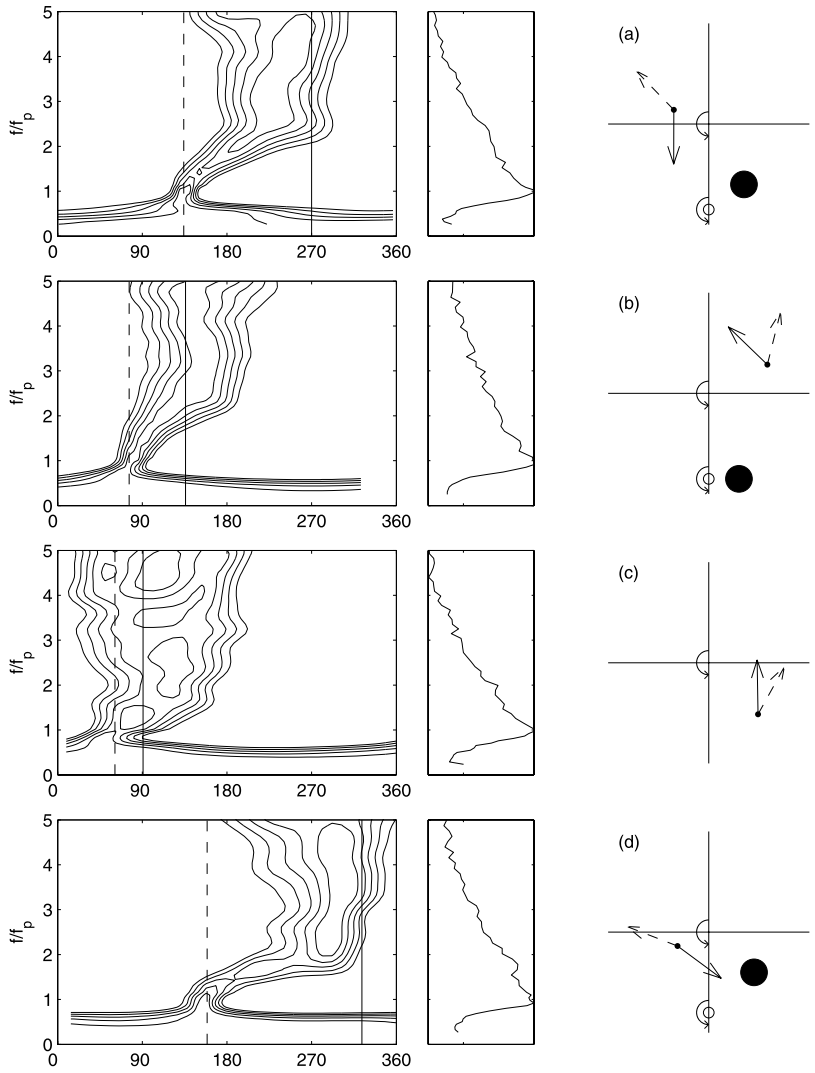

Figure 5. Examples of the directional spreading function, $D(f, \theta)$ for each quadrant of a hurricane. For each quadrant, the panel to the left shows D contoured in f, θ cartesian space. At each frequency, D has been normalized to have a maximum value of one. Contours are drawn 0.9, 0.8, 0.7, 0.6 and 0.5. The vertical dashed line shows the dominant wave direction and the vertical solid line the local wind direction. To the right of the spreading function the one-dimensional frequency spectrum is shown. For these one-dimensional spectra, the energy scale is logarithmic, with the maximum ordinate being 1.0 and the minimum 10^{-3}. The panels to the extreme right show the corresponding position of the measurement in the quadrant under consideration (small solid dot). The dominant wave direction is shown by the dashed arrow and the local wind direction by the solid arrow. At the time of the measurement, the hurricane is located at the centre of the "cross" shown on the panel. The open circle below the cross shows the estimated position of the centre of the hurricane at the time when the dominant waves at the measurement location were generated. The large solid circle to the right of this point shows the approximate region in which these dominant waves were generated. The system is shown for the Northern Hemisphere (i.e. anti-clockwise circulation).

with the waves having been locally generated, rather than remotely generated swell.

5.4. Left-Rear Quadrant

[37] Figure 5d shows a case for the left-rear quadrant. The difference in direction between the local wind-sea and the dominant waves is approximately 170°. As with the left-forward quadrant, the generation region for the dominant waves, appears to be in the right-forward quadrant, ahead of the intense-wind crescent. This region is rotated slightly further anti-clockwise compared to the generation region for the left-forward quadrant. Again, this is consistent with the maximum wind region for which waves could propagate to the measurement location.

6. Parametric Representation of Spreading Function

[38] The MLM (5), used to determine the directional spreading functions is model-independent, in that the direc-

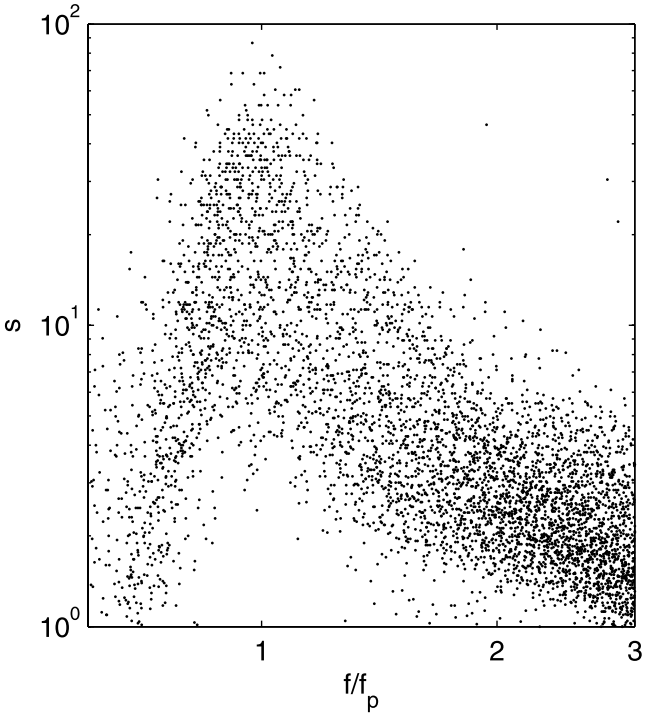

Figure 6. Values of the exponent s from the $\cos^{2s}\theta/2$ model, as a function of f/f_p. Data from all of the hurricanes in the database are shown (a total of 278 spectra).

tional form is not constrained to a particular form (in contrast to the FEM). To present the results in a summary form, it is, however, convenient to fit a simple model to the spreading function. There are three likely candidates for such a form; the $\cos^{2s}\theta/2$ model of *Longuet-Higgins et al.* [1963], the $\mathrm{sech}^2\theta$ model of *Donelan et al.* [1985] and the integral parameter of *Babanin and Soloviev* [1998]. Noting both the statistical variability and the complexity of the skewed spectra, any of these models could be used. As the *Longuet-Higgins et al.* [1963] model is more commonly used, it has been adopted for this purpose.

[39] For each of the spectra, the function $D(\theta) = \cos^{2s}(\theta - \theta_m)/2$ was fitted at each frequency, where θ_m is the angle at which the function is a maximum at that frequency. The value of s at each frequency was determined by matching the "half power" points of the directional distribution, D.

[40] Figure 6 shows the resulting values of s, as a function of f/f_p, for all of the spectra. Although there is significant scatter in the data, it is clear that the directional spreading function has many of the characteristics of directional spreading functions from uni-directional wind cases [e.g., *Mitsuyasu et al.*, 1975; *Hasselmann et al.*, 1980; *Donelan et al.*, 1985; *Babanin and Soloviev*, 1998]. The directional spectra are narrowest at the spectral peak (high values of s) and broaden both above and below the peak frequency (lower values of s).

[41] In order to reduce the scatter in Figure 6, the data were allocated to bins of $\pm 0.1 f/f_p$, and all values in each bin averaged. The mean values and plus/minus one standard deviation about the means are shown in Figure 7. The mean values clearly show the classical "tent" structure common for uni-directional wind fields. Hence, despite the complex directionally skewed spectra within hurricanes, the variation of width follows a similar form to uni-directional cases. A fit to the data yields

$$s(f) = \begin{cases} 20\left(\dfrac{f}{f_p}\right)^{4.5} & \text{for } \dfrac{f}{f_p} < 1 \\ 20\left(\dfrac{f}{f_p}\right)^{-2.4} & \text{for } \dfrac{f}{f_p} > 1 \end{cases} \tag{15}$$

Equation (15) represents an average over all sectors of the hurricane, and it was investigated whether the value of s varied depending on the sector. Within the significant data scatter, there was no clear trend. There was some suggestion that values of s were larger in the forward quadrants of the hurricane, with the smallest values in the right-rear quadrant. Such a result would be consistent with the forward quadrants being dominated by remotely generated swell and the right-rear quadrant being more locally generated, as noted above. This result should, however, be treated with caution as the trend was not clearly defined.

[42] There are few comparable measurements from hurricanes with which to compare (15). The scanning radar

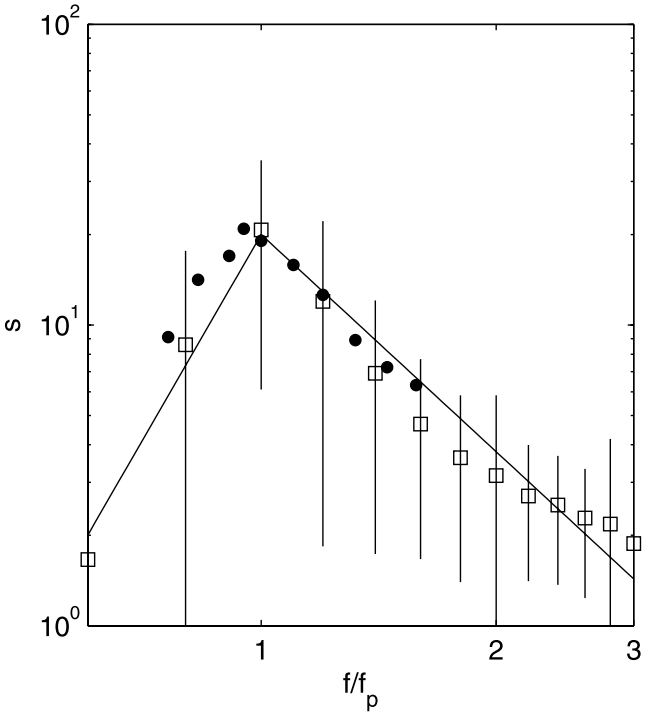

Figure 7. Mean values of the exponent s from the $\cos^{2s}\theta/2$ model, as a function of f/f_p. The data in Figure 6 were binned into segments of $\pm 0.1 f/f_p$ and the mean for the bin calculated. These mean values are shown by the open squares. Plus/minus one standard deviation about these mean values are shown by the vertical "error" bars. The solid lines show the parametric fit to the data represented by (15). The solid dots show approximate values of s, calculated by *Young et al.* [1996] for the fetch-limited uni-directional data of *Donelan et al.* [1985].

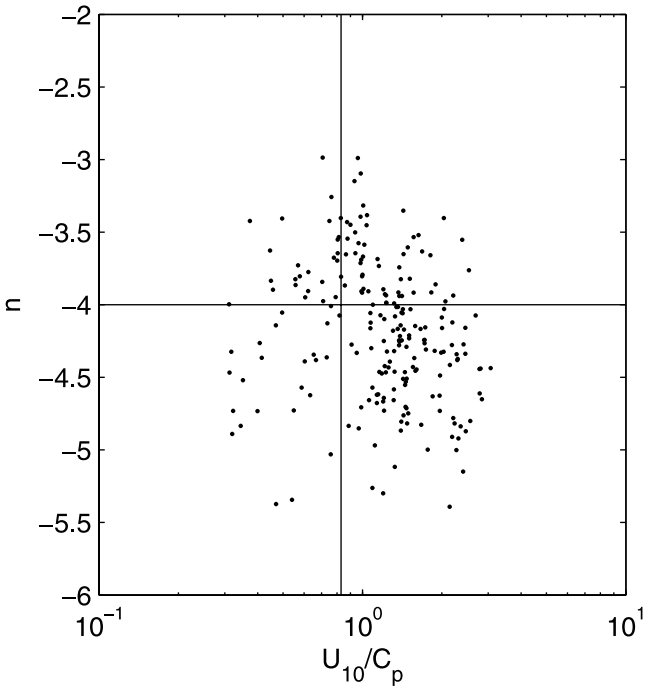

Figure 8. Values of the high frequency exponent n of (3) as a function of the inverse wave age, U_{10}/C_p. The vertical line drawn at $U_{10}/C_p = 0.83$ is the demarcation between swell and wind-sea proposed by *Donelan et al.* [1985]. The horizontal line is drawn at $n = -4$.

altimeter (SRA) results of *Wright et al.* [2001] [see also *Ochi*, 2003] from *Hurricane Bonnie* indicate that the directional spread of the dominant waves is narrow, with energy being largely contained within approximately ±20° of the mean. Assuming that this statement can be interpreted as the width of the half-power points of the directional distribution, a width of ±20° is equivalent to $s = 23$. This is consistent with (15), which yields $s = 20$ at the spectral peak (i.e. the dominant waves). It is interesting to compare the present results with those obtained under uni-directional wind conditions [e.g., *Mitsuyasu et al.*, 1975; *Hasselmann et al.*, 1980; *Donelan et al.*, 1985; *Babanin and Soloviev*, 1998]. Both *Mitsuyasu et al.* [1975] and *Hasselmann et al.* [1980] obtained spreading functions with $s \approx 11$ at the spectral peak, indicating a broader directional spread. It is interesting to note that the exponent of decay of s with f/f_p for these uni-directional studies is almost identical with (15). For example, *Mitsuyasu et al.* [1975] reports a high frequency exponent of 5 and a low frequency exponent of −2.5. This compares with 4.5 and −2.4, respectively for (15).

[43] *Donelan et al.* [1985] adopted a $\mathrm{sech}^2\theta$ model, so it is not directly comparable. *Young et al.* [1996] have, however, recast the results of *Donelan et al.* [1985] into an approximate $\cos^{2s}\theta/2$ form, obtaining values at the spectral peak of $s \approx 20$, as for (15). These recast *Donelan et al.* [1985] results are presented in Figure 7 for comparison. The agreement between the hurricane data and the uni-directional wind field data is remarkably good. *Babanin and Soloviev* [1998] used an integral width parameter, in preference to the exponent s, to represent the spectral width. For the case of $f/f_p = 1$ and $U_{10}/C_p = 1$, this formulation yields an equivalent value of $s = 19.4$, in excellent agreement with (15).

[44] The fact that the *Mitsuyasu et al.* [1975] and *Hasselmann et al.* [1980] results are broader than either *Donelan et al.* [1985], *Babanin and Soloviev* [1998] or the present result is not surprising. These studies both used the FEM to analyse their pitch-roll buoy data. As pointed out by *Young* [1994], and noted for the present data set, the FEM produces results which are artificially broad. It is also important to place into context what a difference in the value of s from 11 to 20, as reported above, really means. A value of $s = 20$ yields a half-power directional width of ±21°, whereas $s = 11$ yields a half-power directional width of ±29°. These differences are not large and probably within the directional resolving power of the recording instruments. As small changes in the directional width give rise to relatively large variation in s, this will also partly explain the significant scatter in Figure 6.

[45] Hence, it can be concluded that despite the fact that the observed hurricane directional spectra are largely dominated by swell at the spectral peak and are directionally skewed, often over angles of greater than 90°, they exhibit many of the same features as uni-directional wind-wave spectra.

7. One-Dimensional Spectra

[46] Although the primary aim of this study was to investigate the directional properties of hurricane wave spectra, the data set also provides an opportunity to investigate the one-dimensional spectrum. Noting that the spectra are almost always uni-modal, the generalized JONSWAP form (3) was adopted for this purpose. Initially, the high-frequency exponent, n was determined by a least-squares fit of the simplified form $F(f) = \beta f^n$ for the frequency range $2f_p < f < 4f_p$. Restricting the fit to this range avoids the effects of peak enhancement near f_p, as well as potential aliasing near the high-frequency Nyquist frequency. Figure 8 shows a plot of n as a function of the inverse wave age U_{10}/C_p. As with the many fetch-limited studies which have investigated this parameter [e.g., *Liu*, 1989], there is scatter in the values of this parameter, and no trend as a function of wave age. The mean value of the data set is $n = -4.2$, and a value of $n = -5$, consistent with JONSWAP [*Hasselmann et al.*, 1973] is clearly not supported by the data. Based on this result, the data appear to be consistent with the *Toba* [1973] and *Donelan et al.* [1985] form where $n = -4$, and this value has been adopted in further analysis.

[47] With the value of $n = -4$ adopted for (3), the remaining spectral parameters, β, σ and γ were determined using a Levenberg-Marquardt non-linear regression model [*Levenberg*, 1944]. The peak frequency was determined using the weighted integral $f_p = \int fF(f)^5 df / \int F(f)^5 df$ [*Young*, 1995].

[48] Figure 9 shows a scatter plot of β as a function of U_{10}/C_p. In addition to the present data, the data of *Young* [1997] are also shown. The *Young* [1997] data consist of an independent data set of one-dimensional spectra from 28 North-West Shelf tropical cyclones (i.e. same geographical location as the present data set). *Donelan et al.* [1985],

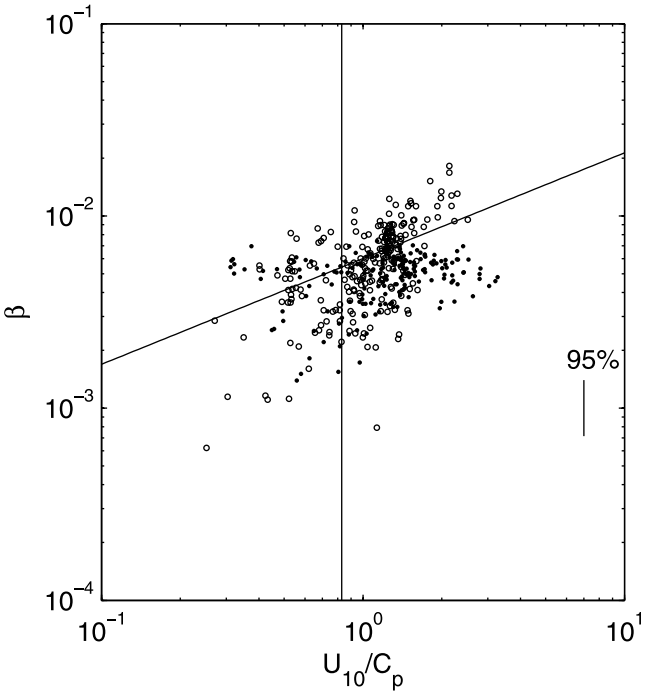

Figure 9. Values of the coefficient, β of (3) as a function of the inverse wave age, U_{10}/C_p. Data from the present study are shown by the solid dots and that from the study of *Young* [1997] by the open circles. Relationship (16), proposed by *Donelan et al.* [1985] for fetch-limited uni-directional winds is shown by the line through the data. The vertical line drawn at U_{10}/C_p = 0.83 is the demarcation between swell and wind-sea proposed by *Donelan et al.* [1985]. The short vertical line to the right of the figure shows the 95% confidence limit appropriate for each of the shown data points.

based on their fetch-limited uni-directional wind field data set, proposed a power law relationship for β:

$$\beta = 0.006\left(U_{10}/C_p\right)^{0.55} \tag{16}$$

Equation (16) is shown in Figure 9 and is a remarkably good fit to the data, again supporting the observation that the spectra are remarkably similar to fetch-limited uni-directional wind field spectra. *Donelan et al.* [1985] have proposed a value of U_{10}/C_p = 0.83 as a limit defining the transition between wind-sea and swell. Values of $U_{10}/C_p <$ 0.83 represent swell. This limit is shown in Figure 9, clearly indicating that much of the combined data set can be categorized as swell, as noted earlier. It is interesting to note that the functional relationship represented by (16) holds, irrespective of whether waves at the spectral peak are being actively forced by the local wind ($U_{10}/C_p > 0.83$) or not ($U_{10}/C_p < 0.83$). It appears that the shape stabilizing processes giving rise to the spectral form are largely independent of local wind forcing.

[49] There is clear data scatter in Figure 9 which may be the result of statistical variability of the data, measurement error, or the limitation of the spectral model, (3). Each of the recorded spectra represents only an approximation to the true spectral form, brought about by the need to use a finite-length record. Thus, each ordinate in the spectrum is a chi-squared variable. As a result, each of the determined spectral parameters will also be an approximation to the true value. Following *Young* [1997], the 95% confidence limits were determined for each of parameters. The confidence limits shown on Figure 9 indicate that the data scatter is consistent with the statistical variability which could be expected as a result of sampling variability.

[50] Figure 10 shows γ as a function of U_{10}/C_p for the combined data set. Many fetch-limited studies have failed to find functional relationships for γ [e.g., *Hasselmann et al.*, 1973]. A notable exception is *Donelan et al.* [1985], who propose

$$\gamma = \begin{cases} 1.7 & \text{for } 0.83 < U_{10}/C_p < 1 \\ 1.7 + 6.0\log_{10}\left(U_{10}/C_p\right) & \text{for } 1 \le U_{10}/C_p < 5 \end{cases} \tag{17}$$

Equation (17) is shown for comparative purposes in Figure 10. There is no clear trend for the value of γ as a function of the inverse wave age, but the results are consistent with the values predicted by (17). Values of γ are typically low (γ ≈ 1–3), characteristic of mature, or well

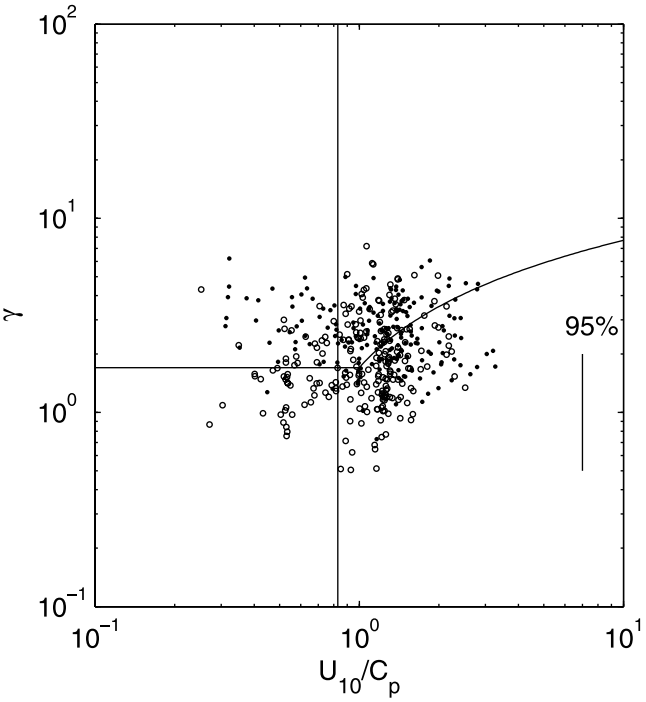

Figure 10. Values of the coefficient, γ of (3) as a function of the inverse wave age, U_{10}/C_p. Data from the present study are shown by the solid dots and that from the study of *Young* [1997] by the open circles. Relationship (17), proposed by *Donelan et al.* [1985] for fetch-limited uni-directional winds is shown by the piece-wise line through the data. The vertical line drawn at U_{10}/C_p = 0.83 is the demarcation between swell and wind-sea proposed by *Donelan et al.* [1985]. The short vertical line to the right of the figure shows the 95% confidence limit appropriate for each of the shown data points.

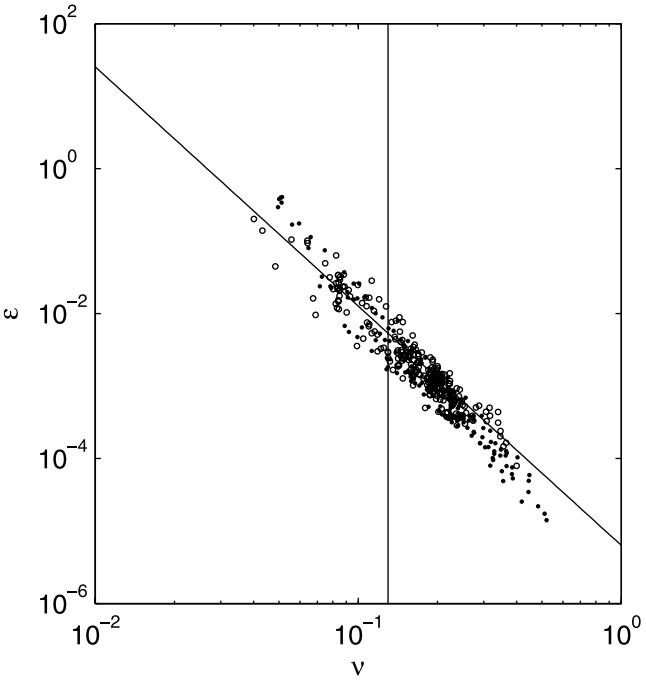

Figure 11. Values of the non-dimensional energy, ε as a function of non-dimensional peak frequency, ν. Data from the present study are shown by the solid dots and that from the study of *Young* [1997] by the open circles. Relationship (18), proposed by *Donelan et al.* [1985] for fetch-limited uni-directional winds is shown by the line through the data. The vertical line drawn at $\nu = 0.13$ is the commonly adopted demarcation between swell and wind-sea.

developed spectra. This is consistent with much of the energy being swell. The scatter which is clear in the data is consistent with the sampling variability, as indicated by the 95% confidence interval shown on this figure.

[51] As with previous fetch-limited studies, no clear trend existed for the values of σ. The mean value for the combined data set was, however, 0.11, consistent with previous fetch-limited studies [e.g., *Donelan et al.*, 1985].

[52] As the spectral parameters defining the hurricane wave spectrum are remarkably consistent with those obtained for relatively simple, fetch-limited cases, it is reasonable to assume that the relationship between the total energy of the spectrum and the peak frequency would be consistent with fetch-limited cases. Both *Donelan et al.* [1985] and JONSWAP [*Hasselmann et al.*, 1973] have proposed similar relationships between non-dimensional energy and non-dimensional peak frequency. The *Donelan et al.* [1985] form is

$$\varepsilon = 6.365 \times 10^{-6} \nu^{-3.3} \tag{18}$$

where $\varepsilon = g^2 E_{tot}/U_{10}^4$ is the non-dimensional energy and $\nu = f_p U_{10}/g$ is the non-dimensional peak frequency (g is the acceleration of gravity and $E_{tot} = \int F(f) df$ is the total energy of the spectrum).

[53] Figure 11 shows ε as a function of ν for the combined data set, together with (18). The agreement between the hurricane data and (18) is remarkable, clearly confirming that the relationship between peak frequency and total wave energy (i.e. H_s) for hurricane wave spectra is consistent with fetch-limited cases.

[54] Equation (18) may seem inconsistent with the observation reported earlier that the peak frequency of spectra, taken from a particular storm, seem to remain quite constant, even as the wave height changes. Equation (18) might be interpreted as indicating the peak frequency would decrease as wave height increases. This is not necessarily the case, as the wind speed, which appears in the non-dimensional parameters also varies in the storm. A simple test can provide an order-of-magnitude assessment. Numerous studies [e.g., *Young and Burchell*, 1996] have shown that the wind speed decreases much more rapidly with distance from the hurricane centre, than does the wave height. Therefore, consider three cases: Case 1: U_{10} = 40 m/s, H_s = 10 m; Case 2: U_{10} = 30 m/s, H_s = 8 m; Case 3: U_{10} = 20 m/s, H_s = 7 m. For these cases, (18) yields: Case1: f_p = 0.083 Hz; Case2: f_p = 0.090 Hz; Case3: f_p = 0.090 Hz. Therefore, although the significant wave height and wind speed vary significantly, the peak frequency remains relatively constant, consistent with observations.

8. Discussion and Conclusions

[55] The data set presented, clearly shows that for all quadrants of the hurricane, with the exception of the right-rear quadrant, the spectra are dominated by swell generated near the intense wind crescent of the hurricane at some earlier point in the passage of the storm. This swell is then "mixed" with the local wind-sea, which often results in a directionally skewed spectrum. Despite this complex generation regime, the spectra exhibit many of the characteristics of directional spectra recorded under much simpler uni-directional wind conditions.

[56] The one-dimensional spectrum conforms to the form proposed by *Donelan et al.* [1985], with a high frequency face proportional to f^{-4}. The parameters representing the one-dimensional spectrum exhibit the same functional dependence on inverse wave age, U_{10}/C_p, as uni-directional wind cases. There is no suggestion that the spectra exhibit a bimodal structure with a low frequency swell peak and a distinct high-frequency wind-sea peak. In addition, the relationship between non-dimensional energy and non-dimensional peak frequency for these hurricane spectra is the same as recorded for uni-directional cases, providing additional evidence that the spectral form has many similarities for the two cases.

[57] The directional spectra are skewed, but there is a continuous smooth transition in direction between the dominant low-frequency swell and the higher frequency components aligned with the local wind direction. There is no tendency for bi-modal distributions to develop in either frequency or direction. Despite the strong directional skewing, the width of the spectrum, as a function of non-dimensional frequency, f/f_p is consistent with uni-directional cases.

[58] Importantly, for many of the hurricane wave spectra, $U_{10}/C_p < 0.83$, and hence there is no active wind forcing at the spectral peak frequency. Hence, a spectral shape consistent with that of uni-directional wind-sea spectra is maintained in the absence of local wind input. This is a

significant result, as it is often assumed that the spectral shape is the result of a balance between wind input, non-linear wave-wave interactions and white-cap dissipation. The present data suggests that, for these mature seas, such a balance is not required to produce such spectral forms. As wind-input is negligible, and dissipation is reactive, rather than active, it is the non-linear wave-wave interaction term which is dominant. This term is apparently capable of reshaping a complex mix of locally generated wind-sea and remotely generated swell to produce spectra, with many of the attributes of uni-directional wind-seas.

[59] Such a result has important consequences for spectral wave modelling, as the actual form of the atmospheric input (and dissipation) is probably not of great importance, only the integral energy input being important. Irrespective of where the input enters the spectrum, the non-linear terms appear capable of redistributing the energy to achieve the same spectral form. Such a dominant role for the non-linear term has previously been proposed by *Zakharov* [2005] and *Badulin et al.* [2005]. In contrast, detailed numerical tests by *Banner and Young* [1994] have indicated that the functional form of all the source terms are important in the detailed development of the spectrum. Based on the present data, this sensitivity does not appear to be the case. This may well indicate that the non-linear wave-wave interaction term is actually stronger than the representations which are implemented in, even the most sophisticated, research models [e.g., *Resio and Perrie*, 1991; *Banner and Young*, 1994].

[60] It should be noted that the spectra within the present database are "mature", with relatively low values of inverse wave age, U_{10}/C_p. For "younger" waves, where input and dissipation may be larger in magnitude, the detailed forms of these terms may still play a role in determining the detailed spectral shape.

[61] In addition to providing insight into the physics of wind-wave evolution, the present analysis also provides a comprehensive description of the directional spectrum under hurricane conditions. With knowledge of the wind field parameters, the wind speed at the point of interest, U_{10} can be estimated. The significant wave height, H_s, and hence E_{tot} can be estimated using a standard parametric model, such as *Young* [1988]. The non-dimensional energy, ε can then be calculated and from (18), the non-dimensional peak frequency, ν, and hence, f_p and C_p determined. The spectral parameters for (3) can be calculated from (16) and (17), and assuming the mean value for σ, the one-dimensional spectrum, $F(f)$ defined.

[62] The direction of the dominant waves (i.e. spectral peak) can be estimated from Figure 4a and the high frequency spectral components above $3f_p$ assumed to align with the local wind direction. Between f_p and $3f_p$ a gradual variation of the mean direction can be assumed. The spectral width at each frequency can be determined from (15). Thus, the full directional spectrum is defined.

[63] Naturally, the accuracy of this approach is limited by the data set available. Although this data set is extensive, undoubted it has its limitations. For instance, it is probable that the directional spreading varies, depending on the quadrant of the storm. One might assume that ahead of the hurricane (forward quadrants), the wave field would be more dominated by swell, and hence the directional spreading would be narrower. There was some suggestion in the data that this may be the case, but no clear trend determined. It may, however, be that the influence of the swell is counteracted by the stabilizing effects of the non-linear wave-wave interactions, forcing the directional spreading back to a universal form, irrespective of the quadrant involved.

[64] *Young* [1988] has shown that both the velocity of forward movement and the maximum wind speed in the storm influence the maximum significant wave height generated. These parameters may also have an impact on the spectral form. It is, however, believed that such influences will be secondary. The primary physics of shape-stabilization, caused by non-linear wave-wave interactions dominating other factors in determining the form of the spectrum, both one-dimensional and directional.

[65] **Acknowledgments.** The data presented in this study were provided by Woodside Energy Ltd, Perth, Western Australia. This significant contribution is gratefully acknowledged. The author would also like to thank Jason McConochie and Stan Stroud for their assistance in supplying the data and manipulating the data formats. The research was partly supported by a Discovery Grant from the Australian Research Council. This support is acknowledged.

References

Antani, J. K. (1981), Mathematical representation of hurricane associated wave spectra, *Rep. UFL/COEL-87-007*, Univ. of Fla.

Babanin, A. V., and Y. P. Soloviev (1998), Variability of directional spectra of wind-generated waves, studied by means of wave staff arrays, *J. Mar. Freshw. Res.*, *49*, 89–101.

Badulin, S. I., A. N. Pushkarev, D. Resio, and V. E. Zakharov (2005), Self-similarity of wind-driven seas, *Nonlinear Processes Geophys.*, *12*, 891–945.

Banner, M. L., and I. R. Young (1994), Modeling spectral dissipation in the evolution of wind waves - Part 1. Assessment of existing model performance, *J. Phys. Oceanogr.*, *24*, 1550–1671.

Beal, R. C., T. W. Gerling, D. E. Irvine, F. M. Monaldo, and D. G. Tilley (1986), Spatial variations of ocean wave directional spectra from the Seasat Synthetic Aperture Radar, *J. Geophys. Res.*, *91*, 2433–2449.

Black, J. L. (1979), Hurricane Eloise directional wave energy spectra, *Proc. 11th Offshore Technol. Conf., OTC 3594*.

Bowyer, P. J., and A. W. MacAfee (2005), The theory of trapped-fetch waves with tropical cyclones – An operational perspective, *Weather Forecasting*, *20*, 229–244.

Capon, J. (1969), High-resolution frequency-wavenumber spectrum analysis, *Proc. IEEE*, *57*, 1408–1418.

Cardone, V. L., and W. J. Pierson (1975), Hindcasting the directional spectra of hurricane generated waves, *Proc. Offshore Technol. Conf., OTC 2332*.

Donelan, M. A., J. Hamilton, and W. H. Hui (1985), Directional spectra of wind-generated waves, *Philos. Trans. R. Soc. London, Ser. A*, *315*, 509–562.

Elachi, C., T. W. Thompson, and D. B. King (1977), Observations of the ocean wave pattern under Hurricane Gloria with Synthetic Aperture Radar, *Science*, *198*, 609–610.

Forristall, G. Z., and E. G. Ward (1980), Directional wave spectra and wave kinematics in hurricanes CARMEN and ELOISE, *Proc. 18th Coastal Eng. Conf.*, *1*, 567–586.

Forristall, G. Z., E. G. Ward, V. J. Cardone, and L. E. Borgmann (1978), The directional spectra and kinematics of surface gravity waves in Tropical Storm Delia, *J. Phys. Oceanogr.*, *8*, 888–909.

Foster, E. R. (1982), JONSWAP spectral formulation applied to hurricane-generated seas, *Rep. UFL/COEL-82/004*, Univ. of Fla.

Gonzalez, F. I., T. E. Thompson, W. E. Brown, and D. E. Weissman (1982), Seasat wind and wave observations of Northeast Pacific Hurricane Iva, August 13, 1978, *J. Geophys. Res.*, *87*, 3431–3438.

Hasselmann, D. E., M. Dunckel, and J. A. Ewing (1980), Directional wave spectra observed during JONSWAP 1973, *J. Phys. Oceanogr.*, *10*, 1264–1280.

Hasselmann, K., et al. (1973), Measurements of wind-wave growth and swell decay during the Joint North Sea Wave Project (JONSWAP), *Dtsch. Hydrogh. Z.*, suppl. A, *8*(12), 95 pp.

Holland, G. J. (1980), An analytical model of the wind and pressure profiles in hurricanes, *Mon. Weather Rev.*, *108*, 1212–1218.
Holt, B., and F. I. Gonzalez (1986), SIR-B Observations of dominant ocean waves near Hurricane Josephine, *J. Geophys. Res.*, *91*, 8595–8598.
Isobe, M., K. Kondo, and K. Horikawa (1984), Extension of MLM for estimating directional wave spectrum, paper presented at Symposium on Description and Modelling of Directional Seas, DHI and MMI, Copenhagen.
King, D. B., and O. H. Shemdin (1978), Radar observations of hurricane wave directions, paper presented at 16th International Conference on Coastal Engineering, Hamburg, Germany.
Levenberg, K. (1944), A method for the solution of certain problems in least squares, *Q. Appl. Math.*, *2*, 164–168.
Liu, P. C. (1989), On the slope of the equilibrium range in the frequency spectrum of wind waves, *J. Geophys. Res.*, *94*, 5017–5023.
Longuet-Higgins, M. S., D. E. Cartwright, and N. D. Smith (1963), Observations of the directional spectrum of sea waves using the motions of a floating buoy, in *Ocean Wave Spectra*, pp. 111–136, Prentice Hall, Upper Saddle River, N. J.
Lygre, A., and H. E. Krogstad (1986), Maximum entropy estimation of the directional distribution in ocean wave spectra, *J. Phys. Oceanogr.*, *16*, 2052–2060.
Mitsuyasu, H., F. Tasai, T. Suhara, S. Mizuno, M. Onkusu, T. Honda, and K. Rukiiski (1975), Observations of the directional spectrum of ocean waves using a cloverleaf buoy, *J. Phys. Oceanogr.*, *5*, 751–761.
Ochi, M. K. (1973), A series of JONSWAP wave spectra for offshore structural design, paper presented at Conference on Behaviour of Structures.
Ochi, M. K. (1993), On hurricane-generated seas, paper presented at 2nd Conference on Ocean Wave Measurement and Analysis, Am. Soc. of Civ. Eng., New Orleans, La.
Ochi, M. K. (2003), *Hurricane-Generated Seas*, 140 pp., Elsevier, New York.
Ochi, M. K., and M. H. Chiu (1982), Nearshore wave spectra measured during Hurricane David, paper presented at 18th International Conference on Coastal Engineering, Cape Town.
Resio, D., and W. Perrie (1991), A numerical study of nonlinear energy fluxes due to wave-wind interactions, *J. Fluid. Mech.*, *223*, 603–629.
Ross, D. (1979), Observing and predicting hurricane wind and wave conditions, collected reprints, pp. 309–321, Atl. Oceanogr. and Meteorol. Lab., Natl. Oceanic and Atmos. Admin., Silver Spring, Md.
Shea, D. J., and W. M. Gray (1973), The hurricane's inner core region, I: Symmetric and asymmetric structure, *J. Atmos. Sci.*, *30*, 1544–1564.
Toba, Y. (1973), Local balance in the air-sea boundary process, *J. Oceanogr. Soc. Jpn.*, *29*, 209–220.
Walsh, E. J., C. W. Wright, D. Vandemark, W. B. Krabill, A. W. Garcia, S. H. Houston, S. T. Murillo, M. D. Powell, P. G. Black, and E. D. Mark (2002), Hurricane directional wave spectrum spatial variation at landfall, *J. Phys. Oceanogr.*, *32*, 1667–1684.
Whalen, J. E., and M. K. Ochi (1978), Variability of wave spectral shapes associated with hurricanes, *Proc. Offshore Technol. Conf., OTC 3228*.
Wright, C. W., E. J. Walsh, D. Vandemark, W. B. Krabill, A. W. Garcia, S. H. Houston, M. D. Powell, P. G. Black, and F. D. Marks (2001), Hurricane directional wave spectrum spatial variation in the open ocean, *J. Phys. Oceanogr.*, *31*, 2472–2488.
Young, I. R. (1988), A parametric hurricane wave prediction model, *J. Waterw., Port Coastal Ocean Eng.*, *114*(5), 637–652.
Young, I. R. (1994), On the measurement of directional wave spectra, *Appl. Ocean Res.*, *16*, 283–294.
Young, I. R. (1995), The determination of confidence limits associated with estimates of the spectral peak frequency, *Ocean Eng.*, *22*(7), 669–686.
Young, I. R. (1997), Observations of the spectra of hurricane generated waves, *Ocean Eng.*, *25*, 261–276.
Young, I. R. (2003), A review of the sea state generated by hurricanes, *Mar. Structures*, *16*, 201–218.
Young, I. R., and G. P. Burchell (1996), Hurricane generated waves as observed by satellite, *Ocean Eng.*, *23*(8), 761–776.
Young, I. R., and G. P. van Vledder (1993), The central role of nonlinear interactions in wind-wave evolution, *Philos. Trans. R. Soc. London, Ser. A*, *342*, 505–524.
Young, I. R., L. A. Verhagen, and S. K. Khatri (1996), The growth of fetch limited waves in water of finite depth. Part III: Directional spectra, *Coastal Eng.*, *28*, 101–122.
Zakharov, V. E. (2005), Theoretical interpretations of fetch-limited wind-drive sea observations, *Nonlinear Processes Geophys.*, *12*, 1011–1020.

I. R. Young, Swinburne University of Technology, P.O. Box 218, Hawthorn, Melbourne, Vic 3122, Australia. (iyoung@swin.edu.au)